EKST

Electrical Transport Analysis using Two Different Hopping Models on $Pr_{0.75}Na_{0.25}Mn_{1-x}Cr_xO_3$ Manganite

N.H. Farizah[1], Suhadir Shamsuddin[2]*

[1][2]*Ceramic and Amorphous Group,
Faculty of Applied Science and Technology,
Universiti Tun Hussein Onn Malaysia, 84600 Pagoh, Johor, MALAYSIA

*Corresponding Author Designation

Abstract: By fitting using the theoretical equation with experimental data of resistivity values, the half-doped for $Pr_{0.75}Na_{0.25}Mn_{1-x}Cr_xO_3$ (x = 0, 0.02 and 0.04) manganite has been analyzed. Small Polaron Hopping (SPH) and Variable Range Hopping (VRH) models were used to fit the electrical resistivity data at the insulating region, which ranged from 300 K to 150 K. The value of hopping energy, E_h, and activation energy, Ea was discovered to change as a result of the influence of Cr content in the sample manganite. Thus, this behavior was proposed as a result of the weakening of the Jahn- Teller (JT) distortion caused by a decrease in the Mn^{3+}/Mn^{4+} ratio, which would influence the Charge Ordering (CO) state. The values of the square linear coefficient (R^2) were examined in order to select the best model for describing electrical resistivity behavior. As a result of the greater value of R^2, it can be shown that Variable Range Hopping (VRH) was chosen as the best model for explaining an electrical resistivity behavior.

Keywords: Electrical Analysis, Small Polaron Hopping, Variable Range Hopping

1. Introduction

Recently, there has been a lot of interest in rare-earth manganite with a general composition. Furthermore, studies on this rare earth manganite have showed that the effects of CMR are comparable to those of a double exchange mechanism (DE), which should be linked to the Jahn-Teller (JT) effect and charge ordering (CO) [1-7]. The manganite exhibits nonconducting behavior due to charge localization and the inhibition of electron hopping from one area to another [8-10]. Cr is a transition metal that is most typically found in the Earth's crust in the metallic state. The impact of Cr^{3+} on $Pr_{0.75}Na_{0.25}Mn_{1-x}Cr_xO_3$. doped with Cr in the Mn region, in particular, reduced the Jahn-Teller distortion (JT) and degraded the metal's behavior. The addition of Cr^{3+} to the Mn location of $Pr_{0.75}Na_{0.25}Mn_{1-x}Cr_xO_3$ could enhance the double exchange method is used to produce ferromagnetic-metallic phases,

which have a direct impact on the Mn-O-Mn network and the spin alignment between metal-insulator transitions (MI) [11-12]. As a consequence, it is clear whether Cr^{3+} activity on manganite could have a significant effect. Furthermore, when Cr^{3+} ions (electrons) are swapped for Mn^{3+} ions, the effect of Jahn-Teller distortion is reduced. This would be accomplished by lowering the Mn^{3+}/Mn^{4+} ratio in a manganite sample, which would alter the charge-ordered (CO) state [13].

This paper also concentrated on further analysing electrical resistivity data to discover the electrical characteristics of $Pr_{0.75}Na_{0.25}Mn_{1-x}Cr_xO_3$ by calculating the activation energy, E_a, hopping energy (E_h), density of states $N(E_F)$ at the Fermi level, and average hop distance (R_h). All of these variables will be calculated separately, with a = 4.5 selected as the localized charging and blocking electron surge of the Boltzmann constant, k_B, and T = 300K [14]. The temperature development of electrical resistance demonstrates that the parent compounds ($x = 0$) exhibit insulating capabilities at lower temperatures. Successive Cr substitutions at the Mn site in $Pr_{0.75}Na_{0.25}Mn_{1-x}Cr_xO_3$ Manganite can cause the metal insulator (MI) transition temperature to be around T_{MI} 180 K for $x = 0.02$ and $x = 0.04$ samples, implying that the double exchange mechanism (DE) is improved as a result of the suppression of the charge order state [15].

In the semiconductor region, the transport mechanism is explained by Variable Range Hopping (VRH) model and Small Polaron Hopping (SPH) model. This model can explain the transport mechanism in manganite. However, most of them are only applied to fit the prominent change of the electrical resistivity curves $\rho(T)$ in a finite temperature region (above or below T_C) [16-17]. The study of this electrical resistivity properties, like the specific heat in the vicinity of the magnetic phase transition, with investigating the values of the universal critical parameters, has not been given the sufficient importance in research projects done on manganite [18]. By conducted the research, which utilized to supply additional information on the electric transport characteristics in order to conduct a robust data analysis. The two hopping models which is SPH and VRH is chosen to fitting for this experiment because it may help us understand the mechanism or behaviour of the electrical transport properties and can choose the best fitting model for the manganite.

Significantly, the results from the SPH-VRH models revealed information regarding the electrical transport mechanism in the insulating region. Using the equation for SPH-VRH models, the data were fitted from experimental onto theoretical. This study is impressive in that it provides a better knowledge of how to determine the greatest model by comparing data analysis. The data analysis in SPH-VRH models that was fitted using equations was compared in order to choose the best models by comparing the linear coefficient (R^2) for SPH and VRH model which models have the value of R^2 close to 1, is the best model to show the electrical resistivity behavior [19].

2. Methodology

The experimental data used in this paper referred from previous worked [16]. The compound $Pr_{0.75}Na_{0.25}Mn_{1-x}Cr_xO_3$ was created using typical solid-state procedures, which focused on the structural properties of electric transport. Small polaron hopping and variable range hopping will be used to examine the electrical transport qualities. This section considers how to reconcile experimental findings with theoretical notions. Two models can be employed to match the electrical transmission test results. The electrical transport parameters of the insulating area were determined using either a tiny polaron hopping or a variable range hopping.

2.1 Experiment Data Fitted with Small Polaron Hopping (SPH)

To gain a better understanding of the electrical behavior in the insulator region of sample $Pr_{0.75}Na_{0.25}Mn_{1-x}Cr_xO_3$ (x=0.00,0.02, and 0.04) at temperatures above T_{MI}, the small polaron hopping (SPH) model was used, as stated by the equations below [16],

$$\rho = BT\exp(E_a/k_BT) \hspace{3cm} Eq.1$$

in which E_a was the activation energy, k_B was the Boltzmann constant, B was the coefficient's resistivity and T is 300 K. Using Sigma Plot version 10, these formulas were utilized to overlay the graph and get the linear coefficient (R^2).

2.2 Experiment Data Fitted with Variable Range Hopping (VRH)

Variable Range Hopping (VRH) was described by the equations below respectively; [16].

$$\rho = \rho_{0m} exp(T_{0m}/T)^{1/4} \qquad Eq.2$$

where ρ is electrical resistivity, ρ_{0m} is the residual resistivity, T_{om} was the Mott's characteristic temperature, and T is Temperature. Using Sigma Plot version 10, these formulae were assessed to fit the graph and the estimated linear coefficient (R^2), and then *Eq.* 1 for SPH and *Eq.* 2 for VRH were compared to establish the optimal model for this analysis. In terms of the VRH model, the following equation gave the fitting graph of the T0m related by the hopping energy, E_h was the density of states, $N(E_h)$ at the fermi level, mean hopping distance, R_h. [16].

$$E_h(T)= \frac{1}{4} k_B(T)^{3/4}(T_{0m})^{1/4} \qquad Eq.3$$

$$N(E_F) = 18a^3/(k_B T_{0m}) \qquad Eq.4$$

$$R_h(T)=(\frac{3}{8})a(T_{0m}/T)^{1/4} \qquad Eq.5$$

where a = 4.5 denoted localization, k_B is Boltzmann's constant, and T = 300 K or the temperature from the data fitting graph that close to room temperature.

3. Results and Discussion

The results and discussion section presents data and analysis of the study. This section described the analysis results obtaining from the experimental data of electrical. This section also describes the techniques of electrical transport characteristics utilizing the SPH-VRH model, in accordance with the study's aim. Then, depending on linear coefficient (R^2) values, what models might be the best for comprehending electrical resistivity data are shown.

3.2 The SPH model

Figure 1 to Figure 3 show a plot of ln (ρ / T) vs 1/T for the $Pr_{0.75}Na_{0.25}Mn_{1-x}Cr_xO_3$ ($x = 0$, 0.02, and 0.04) sample. SPH showed data was computed utilizing *Eq1*. *Eq* 1 provided information on activation energy *(Ea)* while using the SPH model for electrical resistivity data analysis. A solid electron phonon coupling event produced by Jahn- Teller (JT) lattice distortion was proposed by the near vicinity of tiny polarons. The fitted parameter for SPH was shown in Table 1. The activation energy levels for 332.0 meV ($x = 0$), 329.0 meV ($x = 0.02$), and 330.0 meV ($x = 0.04$) grew as the Cr material increased. The activation energy was raised from 329.0 meV for $x = 0.02$ to 330.0 meV for $x = 0.04$. This behavior might be advocated in order to promote charge carrier delocalization. Increased Cr-doped concentrations impaired the Jahn- Teller (JT) interaction due to the impact of Cr^{3+} on Mn^{3+} and the lowered Mn^{3+}/Mn^{4+} ratio. Previous study found that the influence of doping particles on Jahn-Teller twisting was attenuated due to a decrease in the Mn^{3+}/Mn^{4+} ratio.

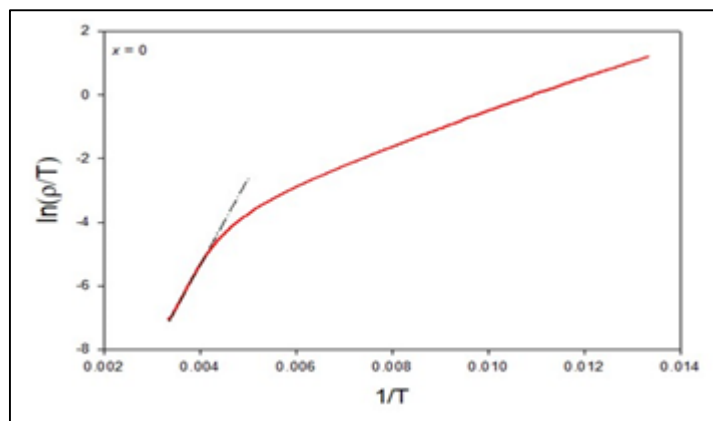**Figure 1: For $x = 0$ manganite sample, plot ln (ρ / T) vs 1/ T. Using the SPH model, solid lines indicated the fitting line.**
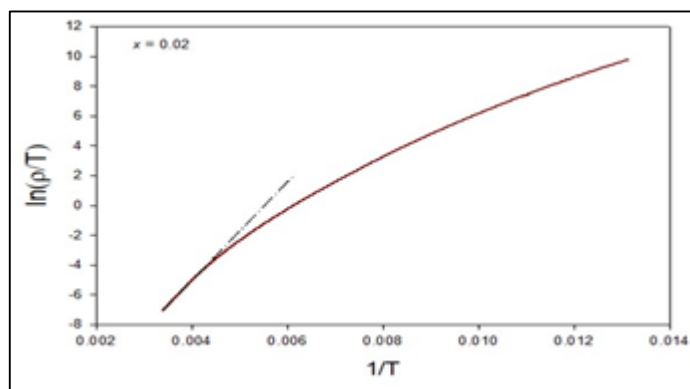

Figure 2: For $x = 0.\,02$ manganite sample, plot ln (ρ / T) vs 1/ T. Using the SPH model, solid lines indicated the fitting line.
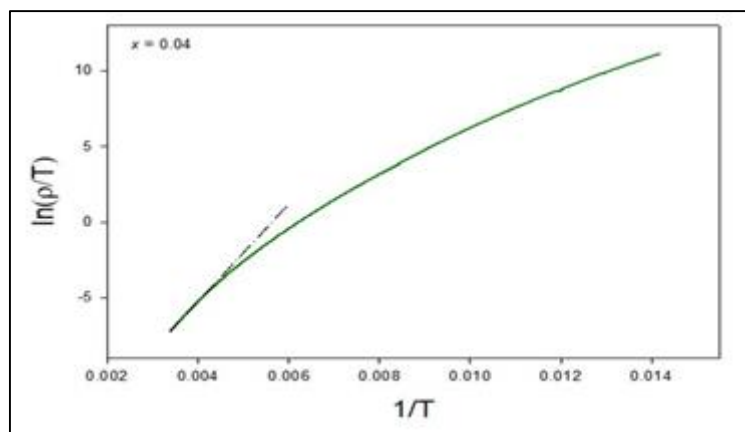

Figure 3: For $x = 0.\,04$ manganite sample, plot ln (ρ / T) vs 1/ T. Using the SPH model, solid lines indicated the fitting line.

Table 1: Fitted parameter for SPH model developed for $Pr_{0.75}Na_{0.25}Mn_{1-x}Cr_xO_3$ sample.

Sample	$\rho = BT\exp(E_\alpha/k_BT)$	
	$R^2 \times 100\%$ (%)	Ea (MeV)
$x = 0$	0.996	332 MeV
$x = 0.02$	0.998	329 MeV
$x = 0.04$	0.998	330 MeV

3.3 The VRH model

Figure 5 through Figure 7 show a plot of ln ρ vs $T^{-1/4}$ for the $Pr_{0.75}Na_{0.25}Mn_{1-x}Cr_xO_3$ ($x = 0$, 0.02 and 0.04). By using VRH demonstrate, strong lines were talked to the fitting line, and information data was calculated using Eq. 2 to find Mott's characteristic temperature, T_{om}. The values of T_{om}, E_h, $N(E_F)$, and R_h obtained from the Eq. 3, 4, and 5 were also computed and organized in Table 2. Table 2 shows that the values of T_{om} for $x = 0$ are 1454 K in the interval and 1800 K ($x = 0.02$). In the $x = 0.04$ case, T_{om}'s esteem was 1564 K. The hopping energy, E_h, values were 9.5924 meV for $x = 0$ in mean time and 10.112 meV for $x = 0.02$, and as can be seen, the E_h values obtained for the $x = 0.04$ sample are 9.7690 meV. Furthermore, mean hopping distance (R_h) values were found, which were 2.5058 for $x = 0$, and 2.6411 for x = 0.02, while the Rh values for x = 0.04 were 2.5499.

After that, the Density of states $(N(E_F))$ values obtained from Table 2 were 1.3087 eV^{-1} cm^{-3} ($x = 0$), 1.0571 eV^{-1} cm^{-3} ($x = 0.02$), and 1.2167 eV^{-1} cm^{-3} ($x = 0.04$) in mean time. It's probable that the electrical resistivity transport qualities caused a trend change. This behavior might be explained by a Cr-doped weaker Jahn-Teller distortion generated by the substitution of Cr^{3+} for Mn^{3+}. The substitution resulted in a decrease in Mn^{3+}/Mn^{4+}, which had an effect on the CO state. This occurrence was caused by the enhanced double exchange (DE) mechanism.
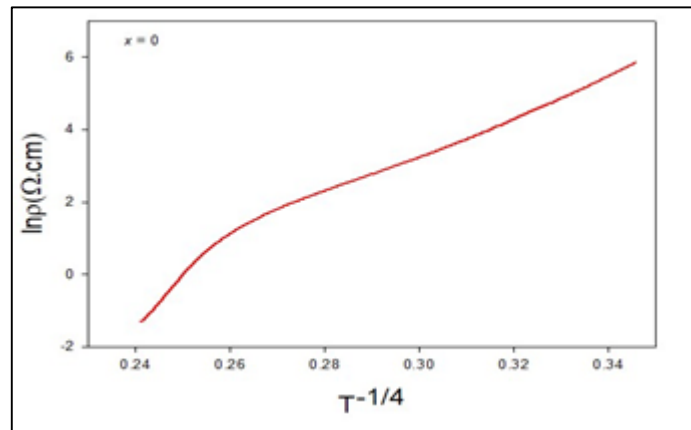
Figure 4: Plot of ln ρ against $T^{-1/4}$ for a manganite sample with $x = 0$. The fitting line was depicted by solid lines using the VRH model.
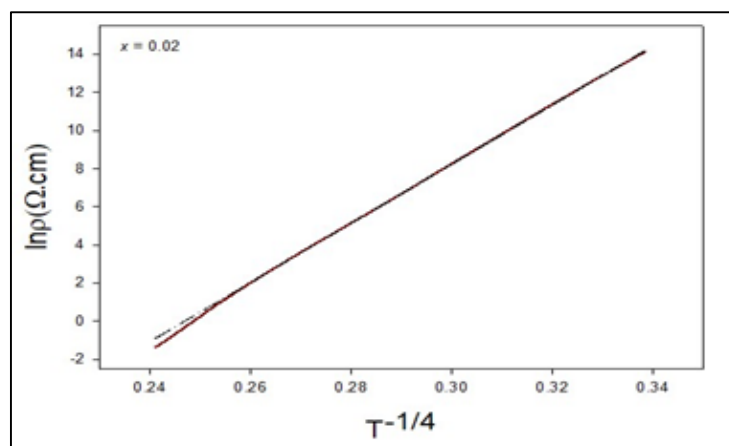
Figure 5: Plot of ln ρ against $T^{-1/4}$ for a manganite sample with $x = 0.02$. The fitting line was depicted by solid lines using the VRH model.
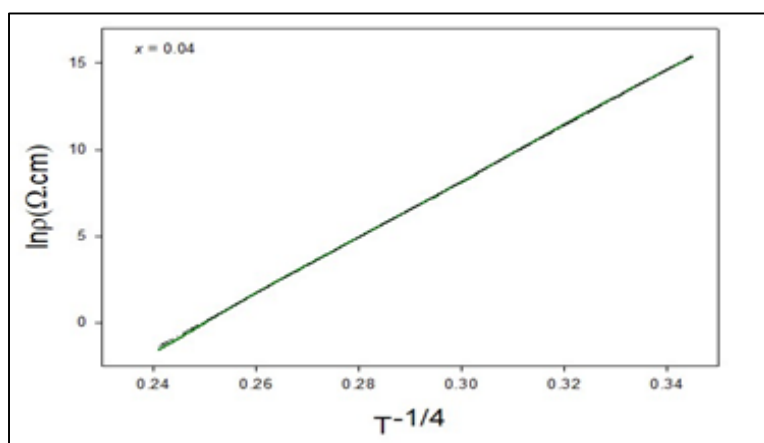

Figure 6: Plot of ln ρ against $T^{-1/4}$ for a manganite sample with $x = 0.04$. The fitting line was depicted by solid lines using the VRH model.

Table 2: Fitted parameter obtained for VRH models fitting for $Pr_{0.75}Na_{0.25}Mn_{1-x}Cr_xO_3$ sample.

Sample	$\rho = \rho_{0m} \exp (T_{0m}/T)^{1/4}$				
	$R^2 \times 100\%$ (%)	T_{om} (K) (10^5)	E_h (300 K) (meV)	R_h (300K) (Å)	$N(E_F)(10^{20})$ (eV^{-1} cm^3)
$x = 0$	0.999	1454	9.5924	2.5058	1.3087
$x = 0.02$	0.999	1800	10.112	2.6411	1.0571
$x = 0.04$	0.999	1564	9.7690	2.5499	1.2167

4. Conclusion

The analysis of electrical transport properties using SPH-VRH models show that, the values of activation energy obtaining from the analysis of SPH model were increase suggestively due to increasing of delocalization of charge carrier as a result of weakening of JT effect. Apart from that, the analysis of VRH model show the value of T_{om} were changed due to increment in Cr-doped and it were improved mean hopping energy also density states at Fermi level that indicate the enhancement of the localization of charge carrier in manganite sample. The electrical resistivity data was found to be a best model to fit the experimental data due to the higher value of R^2.

Acknowledgement

References

[1] M. Arifin, N. Ibrahim, Z. Mohamed, A. K. Yahya, N. A. Khan, & M. N. Khan, "Revival of Metal-Insulator and Ferromagnetic-Paramagnetic Transitions by Ni Substitution at Mn Site in Charge-Ordered Monovalent Doped $Nd_{0.75}Na_{0.25}MnO_3$Manganites", (*Journal of Superconductivity and Novel Magnetism*, *31*(9), 2851–2868). 2018.

[2] N. Asmira, N. Ibrahim, Z. Mohamed, & A. K. Yahya, "Effect of Cr^{3+} substitution at Mn-site on electrical and magnetic properties of charge ordered $Bi_{0.3}Pr_{0.3}Ca_{0.4}MnO_3$ manganite " (*Physica B: Condensed Matter*, *544*, 34–46). 2018

[3] M. Azhar, & M. Mostovoy, "Incommensurate Spiral Order from Double-Exchange Interactions"(*Physical_Review_Letters*,*118*(2),1–5). 2017

[4] A. Banerjee, S. Pal, & B. K. Chaudhuri, "Nature of small-polaron hopping conduction and the effect of Cr doping on the transport properties of rare-earth manganite $La_{0.5}Pb_{0.5}Mn_{1-x}Cr_xO_3$" (*Journal of Chemical Physics*, *115*(3), 1550–1558. 2001.

[5] R.W. Day, D. K. Bediako, M. Rezaee, L. R. Parent, G. Skorupskii, M. Q. Arguilla, C. H. Hendon, L. Stassen, N. C. Gianneschi, P. Kim, & M. Dincă, "Single Crystals of Electrically Conductive Two-Dimensional Metal-Organic Frameworks: Structural and Electrical Transport Properties" (*ACS Central Science*, *5*(12), 1959–1964). 2019.

[6] P. G. De Gennes, "Effects of double exchange in magnetic crystals". (*Physical Review* (*118*(1), 141–154). 1960.

[7] J. Epp, "X-Ray Diffraction (XRD) Techniques for Materials Characterization". (In *Materials Characterization Using Nondestructive Evaluation (NDE) Methods*. Elsevier Ltd.) 2016.

[8] J. Fontcuberta, B. Martínez, A. S. Seffar, Piñol, J. L. García-Muñoz, & X. Obradors, "Colossal magnetoresistance of ferromagnetic manganites: Structural tuning and mechanisms" (*Physical Review Letters*, *76*(7), 1122–1125). 1996.

[9] M. Johnsson, & P. Lemmens, "Crystallography and Chemistry of Perovskites" (*Handbook of_ Magnetism and Advanced Magnetic Materials*, *4*, 1–9). 2007.

[11] J. Fang, "Influence of Bi3 doping on electronic transport properties of $La_{0.5-x}Bi_xCa_{0.5}MnO_3$ manganites" (Physica B: Condensed Matter, 406(6–7), 1312–1316). 2011.

[12] A. Majeed, A. Zeeshan, & T. Hayat, "Analysis of magnetic properties of nanoparticles due to applied magnetic dipole in aqueous medium with momentum slip condition" (Neural Computing and Applications, 31(1), 189–197). 2019.

R. K. Misra, B. Cohen, & L. Etgar, "Low-Dimensional Organic–Inorganic Halide Perovskite: Structure, Properties, and Applications" (ChemSusChem, 10(19), 3712–3721). 2017.

[13] Z. X. Nie, Ouyang, C. Y. Chen, J. Z. Zhong, Z. Y. Du, Y. L Liu, D. S., Shi, S. Q., & Lei, M. S. " First principles study of Jahn-Teller effects in Li_xMnPO_4". (Solid State Communications, 150(1–2), 40–44). 2010.

[14] L. A. Ponomarenko, A. N. Vasil, & Y. A. Velikodny, "Magnetic properties of Cu" (V O. 288, 1459–1460). 2000.

[15] Rabiatul Adawiyah. "Comparative Study on Structural, Electrical Transport and Magnetic Properties of Cr - Doped in Charge - Ordered" (7, 4–7). 2018

[16] N. Sankaranarayanan, & M. S. Ramachandra Rao, "Role of double exchange interaction on the magnetic and electrical properties of $Pr_{0.8}Sr_{0.2}MnO_3$ ferromagnetic insulating manganite". (Journal of Applied Physics, 99(8), 3–6). 2006.

[17] R. Rozilah, N. Ibrahim, Z. Mohamed, A. K. Yahya, N. A. Khan, & M. N. Khan, "Inducement of ferromagnetic-metallic phase in intermediate-doped charge-ordered $Pr_{0.75}Na_{0.25}MnO_3$ manganite by K^+ substitution" (Physica B: Condensed Matter, 521(June), 281–294). 2017..

[18] A. S. B. Ruyan, & G. Rustum, 2000. Plugin-Fulltext-2. 3–26. D. Viehland, S. J. Cross, & M. Wuttig, "Deviation from Curie-Weiss behavior in relaxor ferroelectrics" (Physical Review B, 46(13), 8003–8006). 1992.

[21] P. Wang, "The general properties and applications of ceramic materials". (Applied Mechanics and Materials, 174–177, 215–218) 2012.

[22] L. Zhang, W. Chen, & J. Yang, "Electrical transport properties of filled $CoSb_3$ skutterudites: A theoretical study" (Journal of Electronic Materials, 38(7), 1397–1401). 2009.